Polymer Chemistry

Accepted Manuscript

This is an *Accepted Manuscript*, which has been through the Royal Society of Chemistry peer review process and has been accepted for publication.

Accepted Manuscripts are published online shortly after acceptance, before technical editing, formatting and proof reading. Using this free service, authors can make their results available to the community, in citable form, before we publish the edited article. We will replace this *Accepted Manuscript* with the edited and formatted *Advance Article* as soon as it is available.

You can find more information about *Accepted Manuscripts* in the Information for Authors.

Please note that technical editing may introduce minor changes to the text and/or graphics, which may alter content. The journal's standard Terms & Conditions and the Ethical guidelines still apply. In no event shall the Royal Society of Chemistry be held responsible for any errors or omissions in this *Accepted Manuscript* or any consequences arising from the use of any information it contains.

ROYAL SOCIETY OF CHEMISTRY

www.rsc.org/polymers

Stereocomplex formation in stereoblock copolymer networks composed of 4-armed star-shaped lactide oligomers and 2-armed ε-caprolactone oligomer

Mitsuhiro Shibata*, Masaya Katoh, Hayato Takase and Ayaka Shibita

Department of Life and Environmental Sciences, Faculty of Engineering,
Chiba Institute of Technology, 2-17-1, Tsudanuma, Narashino, Chiba 275-0016, Japan.
E-mail: mitsuhiro.shibata@p.chibakoudai.jp; Tel: +81 47 478 -423

Abstract

Stereoblock copolymer networks were prepared by reactions of methylenediphenyl 4,4'-diisocyanate (MDI) with hydroxy-terminated 4-armed star-shaped L-lactide and D-lactide oligomers (H4LLAO and H4DLAO) with degree of polymerization per one arm, n = 15 in the presence and absence of hydroxy-terminated 2-armed ε-caprolactone oligomer (H2CLO). Thermal and mechanical properties of the MDI-bridged stereoblock copolymer networks (MH-4scLAO/2CLOs 100/0, 75/25, 50/50, 25/75 and 0/100) were compared with those of a simple H4LLAO/H4DLAO blend (H4scLAO) and MDI-bridged homochiral (hc) networks of H4LLAO and H4DLAO (MH4LLAO and MH4DLAO). X-ray diffraction and differential scanning calorimetric analyses revealed that stereocomplex (sc) crystallites are formed without any hc crystallization for MH-4scLAO/2CLOs and H4scLAO, and that MH4LLAO and MH4DLAO are amorphous. The melting temperatures of sc crystallites for MH-4scLAO/2CLOs were much higher than those of hc crystallites of H4LLAO and H4DLAO, while the values were slightly lower than that of H4scLAO. Elongations at break and tensile toughnesses of MH-4scLAO/2CLOs (75/25, 50/50 and 0/100) were much higher than those of MH4LLAO and MH4DLAO.

1. Introduction

Poly(lactide) (PLA) is a bio-based, biodegradable, and biocompatible polyester, which has strength and elastic modulus comparable to those of conventional petroleum-based polymers such as poly(ethylene terephthalate) and polystyrene.[1] PLA has attracted increasing attention

in recent years as the environmentally benign and biomedical materials usable for agriculture, automobile, diary commodities, tissue engineering and controlled drug delivery etc.[2-4] Unfortunately, the application of PLA has been limited because of its poor thermal resistance and fracture toughness as compared with conventional polymers. Therefore, a great deal of efforts has been made to modify the properties of PLA in both industry and academia.[5,6] Regarding the improvement of thermal resistance, formation of stereocomplex (sc) crystallites between poly(L-lactide) (PLLA) and poly(D-lactide) (PDLA) has been proven to be one of the most effective methods to enhance the properties of PLA.[7-11] The stereocomplex crystallites are reported to show a melting temperature (T_m) approximately 50 °C higher than that of PLA homochiral (hc) crystallites.[9] Moreover, the sc-PLA exhibits better mechanical strength and hydrolysis resistance than hc crystalline PLA.[9,11] Since the first report on sc-PLA by Ikada et al.,[8] sc-PLA derivatives having a variety of macromolecular architectures, such as stereo-block copolymers having linear,[12-15] cyclic,[16] brush[17] and star-shaped[18,19] structures, and polymer blends having cyclic,[20] comb[21] and star-shaped[22-34] structures have been reported in past studies. In particular, star-shaped polymers have gathered much attention, because the polymer properties, such as T_m, glass transition temperature (T_g) and viscosity, can be varied by modulating the degree of branching and arm length of the star-shaped polymers.[35] For example, Biela et al. reported enhanced melt stability of star-shaped sc-PLA with 13-arms or more.[22] Purnama et al. reported that 8-armed star-shaped sc-PLAs with a polyhedral oligomeric silsesquioxane core had higher melt stability than 8-armed star-shaped sc-PLAs with a tripentaerythritol core.[31] Isono et al. reported that solvent cast samples of 3,4 and 5-armed star shaped PLAs having both PLLA and PDLA arms formed sc-crystals without any homochiral crystallization.[18] Tsuji and Yamashita reported highly accelerated sc crystallization by blending star-shaped 4-armed stereo diblock PLAs with PDLA and PLLA cores.[34] However, the improvement of fracture toughness for sc-PLAs has never been reported in the past studies.

On the other hand, the fracture toughness of PLAs has been improved by various methods leading to the introduction of flexible chains[36] such as polymer blend,[37-44] copolymerization[45-47] and crosslinking.[48-51] Recently, we have reported that semi-interpenetrating polymer network (semi-IPN) composed of PLA and polymer network formed by the reaction of hydroxy-terminated 4-armed star-shaped ε-caprolactone oligomer and a diisocyanate has a considerably higher tensile toughness than pure PLA.[52] We also

reported that a similar type of semi-IPN composed of poly(ε-caprolactone) (PCL) and a polymer network based on 4-armed star-shaped L-lactide oligomer has a higher tensile toughness than pure PLA.[53] In this study, as a new strategy to improve both the T_m and toughness of star-shaped PLA, 4-armed star-shaped sc-PLAs with copolymer network structure containing flexible PCL chain are investigated. Regarding the sc-PLAs having network structure, Bai et al. recently reported that sc-PLAs partially crosslinked with a trace amount (0.1-0.5 wt%) of triallyl isocyanurate (TAIC) had good melt stability.[54] Melt stability and sc-crystallization behavior are also investigated in this study for the fully crosslinked sc-PLA polymer networks which have a much higher crosslinking density than the partially crosslinked sc-PLAs with TAIC.

2. Experimental section

2.1 Materials

Pentaerythritol (PERT) and methylenediphenyl 4,4'-diisocyanate (MDI) were purchased from Tokyo Chemical Industry Co., Ltd. (Tokyo, Japan). Tin (II) bis(2-ethylhexanoate) ($Sn(Oct)_2$) was purchased from KISHIDA CHEMICAL Co. Ltd. (Osaka, Japan). L-Lactide (LLA, >99%) and D-lactide (DLA, >99%) were purchased from Musashino Chemical Laboratory, Ltd. Hydroxy-terminated 2-armed ε-caprolactone oligomer (H2CLO) whose catalogue name is polycaprolactone diol with a number-averaged molecular weight (M_n) ~2,000 was purchased from Sigma-Aldrich Corporation (St. Louis, MO, USA). The H2CLO is a diglycerol-initiated 2-armed ε-caprolactone oligomer with a degree of polymerization per one arm, m = ca. 8.4 (Scheme 1). 1,2-Dichloroethane (DCE) was purchased from Kanto Chemical Co. Inc. (Tokyo, Japan). PLLA [REVODE® 110, density 1.25 g cm^{-3}, D-content 2.5%, melt flow rate (190 °C, 2.16 kg) 5 g/10 min] was purchased from Zhejiang Hisun Biomaterials Co., Ltd (Taizhou, China). All the reagents were used without further purification.

2.2 Synthesis of H4LLAO or H4DLAO

Synthesis of hydroxy-terminated lactide oligomers had been previously reported by several groups.[53, 55-59] We used chlorobenzene as a reaction solvent in order to avoid the sublimation of lactide (LA).[53,59] A typical synthetic procedure of H4DLAO with a theoretical degree of polymerization of lactate unit per one arm, n = 20.6 in this study is as follows: PERT (2.32 g, 17.0 mmol), DLA (100.7 g, 699 mmol) and chlorobenzene (50 mL) were put into a nitrogen

purged three-necked flask. The mixture was heated to 150 °C until complete dissolution of PERT, and then $Sn(Oct)_2$ (1.03 g, 2.54 mmol) was added into the flask. The resulting mixture was stirred at 150 °C under a nitrogen atmosphere for 24 h. The cooled reaction mixture was added to 300 mL of methanol with stirring. The formed precipitate was filtered, washed with methanol several times and dried at 80 °C in vacuo to give H4DLAO as a white powder (78.3 g, 76%). ^{1}H-NMR δ_H (400 MHz; DMSO-d_6; Me_4Si) 5.23 (m, (n–1)H; repeating (C=O)C*H*), 4.3-4.1 (m, 3H; CCH_2+terminal(C=O)C*H*), 1.50 (bs, 3(n–1)H; repeating CH_3), 1.32 (bs, 3H; terminal CH_3). The degree of polymerization (n) per one arm measured by ^{1}H-NMR method was 15.5 (see Figure S1 in Electronic Supplementary Material). FT-IR ν_{max}/cm^{-1} 3530w (OH), 2988w (CH) and 1759s (CO) (see Figure S3). H4LLAO was also synthesized in 72% yield by the same procedure as that of H4DLAO except to use LLA instead of DLA. The value of n for H4LLAO was 15.1 (see Figure S2).

2.3 Preparation of stereocomplex polymer blend of H4LLAO and H4DLAO (H4scLAO)

A solution of H4LLAO (2.24 g, 0.497 mmol) and H4DLAO (2.24 g, 0.491 mmol) in DCE (50 mL) was poured into a petri dish (diameter: 100 mm) made of poly(tetrafluoroethylene), and dried at 60 °C for 24 h, and then 130 °C for 4 h in an electric oven. The obtained H4scLAO was white powder.

2.4 Typical synthetic procedure of MDI-bridged polymer network

A solution of H4LLAO (1.01 g, 0.224 mmol), H4DLAO (1.01 g, 0.221 mmol), MDI (0.307 g, 1.23 mmol) and H2CLO (0.67 g, 0.335 mmol) in DCE (50 mL) was poured into a petri dish (diameter: 100 mm) made of poly(tetrafluoroethylene). The molar ratio of OH/NCO in the mixture was fixed to 1/1. The mixture was dried at 60 °C for 24 h, and then 130 °C for 4 h in an electric oven. The obtained MDI-bridged stereocomplex network of H4LLAO, H4DLAO and H2CLO (MH-4scLAO/2CLO) with the feed weight ratio of (H4LLAO+H4DLAO)/H2CLO 75/25 (thickness: ca. 0.4 mm) was peeled off from the petri dish. MH-4scLAO/2CLO (100/0, 50/50, 25/75 and 0/100) films were also prepared by a similar method. MH-4scLAO/2CLO 100/0 and MH-4scLAO/2CLO 0/100 are also abbreviated as MH4scLAO and MH2CLO, respectively. As a comparison, the reaction product of H4LLAO or H4DLAO with MDI (MH4LLAO or MH4DLAO) was also prepared by a similar method.

2.5 Characterization and measurements

Proton nuclear magnetic resonance (^{1}H-NMR) spectra were recorded on a Bruker AV-400 (400 MHz) (Madison, WI, USA) using dimethyl sulfoxide-d_6 (DMSO-d_6) and tetramethylsilane as a solvent and an internal standard, respectively. Fourier transform infrared (FT-IR) spectra were recorded at room temperature in the range from 4000 to 700 cm^{-1} on a Shimadzu (Kyoto, Japan) FT-IR 8400s by the attenuated total reflectance (ATR) method. The IR spectra were acquired using 50 scans at a resolution of 4 cm^{-1}. X-ray diffraction (XRD) analysis was performed at ambient temperature on a Rigaku (Tokyo, Japan) RINT-2100 X-ray diffractometer at a scanning rate of 2.0° min^{-1}, using Cu Kα radiation (wavelength, λ = 0.154 nm) at 40 kV and 14 mA. All scans were in the range $5° \le 2\theta \le 30°$ at a scanning rate of 1.0° min^{-1} and a step size of 0.01°. The crystallinity values of the hc oligolactide crystallines ($\chi_{c,hc}$) and stereocomplex oligolactide crystallines ($\chi_{c,sc}$) for H4LLAO, H4DLAO and MH4scLAO were determined by a simplified method using XRD profiles. Namely, for a 2θ range of 5-30°, the crystalline peak areas for the hc crystallites at 2θ values around 16, 19° and 22°, and for the sc crystallines at 2θ values around 12, 20° and 24° relative to the total area between a diffraction profile and baseline were used to estimate $\chi_{c,hc}$ and $\chi_{c,sc}$, respectively.[34,60] Dynamic mechanical analysis (DMA) of the rectangular plates (40 × 8 × 0.4 mm^3) was performed on a Rheolograph Solid instrument (Toyo Seiki Co., Ltd., Tokyo, Japan) under an atmosphere of air with a chuck distance of 20 mm, a frequency of 1 Hz and a heating rate of 2 °C min^{-1}, based on ISO 6721-4:1994 (Plastics-Determination of dynamic mechanical properties, Part 4: Tensile vibration−Non-resonance method). Differential scanning calorimetry (DSC) measurements were performed on a Perkin-Elmer (Waltham, MA, USA) Diamond DSC in a nitrogen atmosphere. The as-prepared samples (8-12 mg) were heated from −100 °C to 230 (or 200) °C at a heating rate of 20 °C min^{-1}, held at the temperature for 3 min to eliminate a thermal history of the sample, and then cooled to −100 °C at a cooling rate of 100 °C min^{-1}. After held at −100 °C for 3 min, the second heating scan was monitored at a heating rate of 20 °C min^{-1}. Glass transition temperature ($T_{g,x}$), cold crystallization temperature ($T_{c,x}$), enthalpy of cold crystallization ($\Delta H_{c,x}$), melting temperature ($T_{m,x}$) and enthalpy of melting ($\Delta H_{m,x}$) for each component (x = LAO or CLO) were determined from the first and second heating curves. The crystallinity of hc or sc oligolactide crystallites ($\chi_{c,LAO}$) was calculated using the following equation:

$$\chi_{c,LAO}(\%) = \left(\frac{\Delta H_{m,LAO}}{w \Delta H^{0}_{m,LAO}} \right) \times 100$$

where w is the weight fraction of MH4LLAO and MH4DLAO, and $\Delta H^{0}_{m,LAO}$ is enthalpy of 100% crystalline hc-PLA (93 J g^{-1}) or sc-PLA (142 J g^{-1}).[9,17] The 5% weight loss temperature (T_5) was measured on a Shimadzu TGA-50 thermogravimetric analyzer. A sample of about 20 mg was heated from room temperature to 500 °C at a heating rate of 20 °C min^{-1} in a nitrogen purge stream at a flow rate of 50 mL min^{-1}. Tensile test of the rectangular specimen (length 40 mm, width 5 mm, thickness 0.4 mm) was performed at 25 °C using a Shimadzu Autograph AG-1 based on the standard method for testing the tensile properties of plastics (JIS K7161:1994 (ISO527-1:1993)). Span length and testing speed were 25 mm and 5 mm min^{-1}, respectively. Five specimens were tested for each set of samples, and the mean values and the standard deviation were calculated.

3. Results and discussion

3.1 Polymer network formation from H4LLAO and/or H4DLAO

First, we estimated a minimum n value of H4LLAO and H4DLAO required for the formation of sc crystallites by the DSC analysis of H4LLAO/H4DLAO mixtures with n = 10 and 15. Only the mixture with n = 15 displayed $T_{m,LAO}$ of sc crystallites. Therefore, we used the H4LLAO and H4DLAO with n = 15 in this study. A similar dependency of molecular weight for the sc formation was reported for blends of high-molecular-weight PLLA and multi-branched PDLA with various molecular weights.[61] In this literature, sc crystallites were formed by use of the multi-branched PDLA with n = 17, while were not formed in case of n = 7. A series of stereoblock copolymer networks, MH-4scLAO/2CLO 100/0, 75/25, 50/50, 25/75, 0/100 were prepared by reactions of H4LLAO, H4DLAO, H2CLO and MDI (Scheme 1). The hc networks, MH4LLAO and MH4DLAO were also prepared by reactions of MH-H4LLAO and H4DLAO with MDI, respectively. All the network samples prepared by a DCE-solution cast method were obtained as relatively tough films, while H4scLAO prepared by the same method using a mixture of H4LLAO and H4DLAO was a white powder sample, indicating that the formation of network structure is important to produce a film sample composed of star-shaped lactide oligomers.

Fig. 1 shows FT-IR spectra of MH-4scLAO/2CLOs compared with those of H4LLAO and MDI. FT-IR spectra of H4DLAO and MH4LLAO (or MH4DLAO) were substantially the same as those of H4LLAO and MH-4scLAO/2CLO 100/0 (i.e. MH4scLAO), respectively (see Figure S3). A weak band at 3530 cm^{-1} due to O–H stretching vibration (ν_{O-H}) observed for H4LLAO and a strong band due to NCO stretching vibration (ν_{NCO}) at 2250 cm^{-1} observed for MDI were almost nonexistent for MH-4scLAO/2CLOs. Although absorption bands characteristic of urethane bond for MH-4scLAO/2CLOs are not so strong because the fraction of urethane bonds formed in the polymer network is a little, new absorption bands of N−H stretching vibration (ν_{N-H}) and N−H bending vibration (δ_{N-H}) were certainly appeared at 3350 and 1533 cm^{-1}, respectively. The latter band at 1533 cm^{-1} contained a shoulder band at 1518 cm^{-1} due to a stretching vibration of carbon-carbon bond of the benzene ring derived from MDI. The band of C=O stretching vibration ($\nu_{C=O}$) at 1744 cm^{-1} for MH4scLAO was a little broader than the corresponding band at 1759 cm^{-1} for H4LLAO, attributable to the fact that the former is composed of oligolactide $\nu_{C=O}$ band at ca. 1760 cm^{-1} and urethane $\nu_{C=O}$ band at ca. 1710 cm^{-1}. MH-4scLAO/2CLO 0/100 (i.e. MH2CLO) exhibited an absorption band at 1722 cm^{-1} as a result of the overlapping of oligocaprolactone and urethane $\nu_{C=O}$ bands. The front edges of $\nu_{C=O}$ band for MH-4scLAO/2CLOs (75/25, 50/50 and 25/75) were split into two as the band is ascribed to oligolactide, oligocaprolactone and urethane C=O vibrations. These results suggest that the reaction of hydroxy group of H4LLAO/H4DLAO and isocyanate group of MDI smoothly proceeded to generate the polymer network having bridged urethane linkages. The formation of polymer networks for MH4LLAO, MH4DLAO and MH-4scLAO/2CLOs (100/0, 75/25, 50/50 and 25/75) were also confirmed by an extraction experiment with chloroform in which all the reactants are soluble. Thus, $100w_1/w_0$ values of MH-4scLAO/2CLOs (100/0, 75/25, 50/50 and 25/75), where w_0 is weight of an original sample and w_1 is weight of the sample dipped in chloroform at room temperature for 1 day and then dried at 40 °C in vacuo, were 113.0%, 101.1%, 92.4% and 41.0%, respectively. Also, MH2CLO completely dissolved in chloroform because the polymer is a linear polymer. The fact that the $100w_1/w_0$ value decreased with increasing feed H2CLO content should be cause by the extraction of branched polymers with a higher fraction of H2CLO-based moiety.

3.2 Stereocomplex formation in stereoblock copolymer networks

Fig. 2 shows XRD profiles of H4LLAO, H4DLAO, MH4LLAO and MH4DLAO. The XRD patterns of H4LLAO and H4DLAO exhibited diffraction peaks of hc crystals at 2θ values of 16.4, 18.6 and 21.9° in a similar manner to PLLA and PDLA.[9,10,62] The $\chi_{c,hc}$ values for H4LLAO and H4DLAO were 47.4% and 34.8%, respectively. The peaks characteristic of hc crystallines were not appeared for MH4LLAO and MH4DLAO, suggesting the formation of polymer network by urethane linkages prevent the hc crystallization. The MH4LLAO and MH4DLAO films which were allowed to stand at room temperature for 1 month displayed small diffraction peaks of hc crystals. A similar suppression of crystallization of the oligolactate chain by crosslinking were reported for the crosslinked 4-armed star-shaped L-lactide oligomers with degrees of polymerization of lactate unit per one arm, n = 3, 5 and 10. [53, 59]

Fig. 3 shows XRD profiles of H4scLAO and MH-4scLAO/2CLOs (100/0, 75/25, 50/50, 25/75 and 0/100). XRD patterns of H4scLAO and MH-4scLAO/2CLO 100/0 (i.e. MH4scLAO) exhibited diffraction peaks at 2θ values of 11.6, 20.3 and 23.7°, corresponding to the (001) planes, (300) and/or (030) planes, and (220) planes of sc crystallites.[63] The $\chi_{c,sc}$ values for H4scLAO and MH4scLAO were 39.3% and 26.2%, respectively. No diffraction peaks due to the hc crystallites were observed in the XRD profiles, suggesting that sc crystallites were selectively formed without the formation of hc crystallites. It is inferred that the sc crystallites of MH-4scLAO were formed accompanied with crosslinking during the solvent evaporation, considering the following previous results on the sc PLA crystallization: 4-armed stereo-miktoarm star-shaped PLAs with M_n of ca. 10 000 formed sc crystals without any trace of hc crystallization by a solution casting method;[18] melt mixing of 6-armed star-shaped PLLA and PDLA with M_n ca 9 000 produced both hc and sc crystals; [22] and partial crosslinking of PLLA/PDLA with triallyl isocyanurate by irradiation considerably suppress the sc crystallization.[54,64] The XRD profiles of MH-4scLAO/2CLOs (75/25, 50/50, 25/75 and 0/100) exhibited the diffraction peaks ascribed to both sc-PLA and oligocaprolactone crystallites. The diffraction peaks at 2θ values at 21.3° and 23.2° corresponds to the (001) and (200) planes of oligocaprolactone crystallites, respectively, [65] the latter of which overlapped by the diffraction peak at 23.7° due to sc-PLA crystallites. The fact that the ratio of peak heights at 20.3° and 21.3° related to sc-PLA and oligocaprolactone crystallites changed proportionally with the composition of MH-4scLAO/2CLO indicated that crystallizations of sc-PLA and oligocaploractone are not disturbed each other.

Fig. 4 shows the first heating DSC curves of H4LLAO, MH4LLAO, H4scLAO, and MH-4scLAO/2CLOs (100/0, 75/25, 50/50, 25/75 and 0/100). In addition, the first heating DSC curves of H4DLAO and MH4DLAO were shown in Figure S4. Table 1 summarizes the data estimated from the first heating DSC curves for all the samples. The $T_{m,LAO}$s based on hc crystals for H4LLAO and H4DLLA were 138.0 and 138.7 °C, respectively. MH4LLAO and MH4DLAO exhibited no $T_{m,LAO}$, indicating that the hc polymer networks are amorphous in agreement with the result of XRD. The $T_{g,LAO}$s (77.9 and 73.8 °C) of MH4LLAO and MH4DLAO were higher than those (52.0 and 59.8 °C) of H4LLAO and H4DLAO, suggesting that the formation of polymer network disturbed the chain mobility. MH-4scLAO/2CLOs (100/0, 75/25, 50/50 and 25/75) displayed the $T_{m,LAO}$s based on sc crystals at around 180 °C, which were much higher than the $T_{m,LAO}$s (138-139 °C) based on hc crystals of H4LLAO and H4DLLA, while were lower than the $T_{m,LAO}$ (196.1 °C) based on sc crystals of H4scLAO. The $\chi_{c,LAO}$s (12-23%) of sc-crystallites for MH-4scLAO/2CLOs (100/0, 75/25, 50/50 and 25/75) were lower than that (33.5%) for H4scLAO in agreement with the trend on $\chi_{c,sc}$ values calculated from XRD profiles. The MH-4scLAO/2CLOs (50/50, 25/75 and 0/100) also displayed $T_{m,CLO}$s at 51-54 °C. $T_{g,LAO}$ (94.4 °C) of H4scLAO was much higher than those (52.0 and 59.8 °C) of H4LLAO and H4DLAO, and was also higher than those (77.9 and 73.8 °C) of MH4LLAO and MH4DLAO. The significant increase of $T_{g,LAO}$ for H4scLAO is interesting when compared with the fact that T_g of the linear sc-PLA prepared by solution casting method of PLLA and PDLA with a weight-averaged molecular weight (M_w) from 5×10^4 to 1×10^5 is 5 °C higher than that of the pure PLLA or PDLA.[11] The increase of $T_{g,LAO}$ for H4scLAO may be caused by disturbance of molecular motion in the amorphous region due to the formation of supramolecular polymer network by sc-crystallization of 4-armed star-shaped oligomers. We could not observe any clear $T_{g,LAO}$s in the first heating DSC thermograms of MH-4scLAO/2CLOs (100/0, 75/25 and 50/50).

Fig. 5 shows the second heating DSC curves of MH-4scLAO/2CLOs (100/0, 75/25, 50/50, 25/75 and 0/100) after cooling at a rate of −100 °C min^{-1} from 230 (or 200) °C to −100 °C. Table 2 summarizes the data estimated from the second heating DSC curves. The fact that the values of $\Delta H_{c,LAO}$ and $\Delta H_{m,LAO}$ were close to each other indicates that the sample before the second heating is almost amorphous. The $T_{c,LAO}$s (83-90 °C) of MH-4scLAO/2CLOs (75/25, 50/50 and 25/75) were much lower than that (122.6 °C) of MH4scLAO, and the former $T_{m,LAO}$s (185-190 °C) were higher than the latter one (167.4 °C). Although $\chi_{c,LAO}$s

(12-20%) of sc-crystallites for MH-4scLAO/2CLOs (75/25, 50/50 and 25/75) were lower than that (22.5%) for MH4scLAO in the first heating scans, the former $\chi_{c,LAO}$s (13-18%) were inversely higher than the latter value (7.1%) in the second heating scans. These results suggest that flexible oligocaprolactone chain of the former sample facilitated sc cold-crystallization of oligolactate chain. It is noteworthy that MH-4scLAO/2CLOs (100/0, 75/25, 50/50 and 25/75) showed no $T_{c,LAO}$s and $T_{m,LAO}$s based on hc crystallites. This is probably caused by the possibility that melted LLA oligomer segment is relatively close to the position of melted DLA oligomer segment because both the segments are incorporated in the polymer network.

3.3 Thermal and mechanical properties of stereoblock copolymer networks

Fig. 6 shows DMA curves of MH-4scLAO/2CLO films (100/0, 75/25, 50/50, 25/75 and 0/100). Tan δ peak temperature corresponding to T_g for MH4scLAO were 78.2 °C, which was much higher than that (55.1 °C) for PLLA reported previously.[52, 59] Tan δ peak temperature for MH2CLO were −38.9 °C, which was much higher than that (−56.3 °C) for PCL reported previously.[52] Tan δ peak temperature (57.8 °C) of MH-4scLAO/2CLO (75/25) was lower than that of MH4scLAO, indicating that the ε-caprolactone oligomer (CLO) segment compatibilized with the LA oligomer (LAO) segment. This result is marked contrast to the fact that poly(DL-lactide)/PCL or PLLA/PCL 70/30 blend prepared by solution casting method displayed two tan δ peaks corresponding to the two components.[66,67] Although DMA measurements of MH-4scLAO/2CLOs (50/50 and 25/75) stopped at around 40 °C because of melting of the CLO segment, two tan δ peaks for the MH2CLO-rich and MH4scLAO-rich segments were observed at −38 to −30 °C and 15 to 30 °C, respectively. These results suggest that excess CLO segments are phase-separated from MH-4scLAO rich segments for the MH-4scLAO/2CLOs with MH2CLO content higher than 25 wt%. The storage modulus (E') of MH-4scLAO/2CLOs (50/50 or 25/75) dropped at around −40 °C due to the glass transition of CLO segments. The E' of MH-4scLAO/2CLOs (75/25) gradually decreased with increasing temperature because of the compatibilization of CLO and LAO segments.

Fig. 7 shows TGA curves of MH4LLAO, MH4DLAO and MH-4scLAO/2CLOs (100/0, 75/25, 50/50, 25/75 and 0/100). The T_5 (246.9 °C) of MH4scLAO was higher than those (234.0 and 229.2 °C) of MH4LLAO and MH4DLAO, indicating the formation of sc

crystallites can improve the heat resistance. T_5 (302.2 °C) of MH2CLO was much higher than that (246.9 °C) of MH4scLAO, in agreement with the observation that T_5 (401.9 °C) of PCL is much higher than that (370.3 °C) of PLA.[52] MH-4scLAO/2CLOs (75/25, 50/50 and 25/75) showed two-step thermodegradation curves, which are caused by the decomposition of LAO and CLO components.

Fig. 8 shows typical stress-strain curves of MH-4scLAO/2CLOs (100/0, 75/25, 50/50, 25/75 and 0/100). Strain (elongation) at break and initial slope (tensile modulus) for MH4scLAO were much lower and higher than those of MH2CLO, respectively, in agreement with the fact that LAO segment is much stiffer than CLO segment. Maximal stress and tensile modulus of MH-4scLAO/2CLO decreased, and inversely elongation at break increased with MH2CLO content. As the toughness is defined as the energy needed to break a sample of unit area and unit length (J m^{-3}), it is given by the area under the stress-strain curve.[52,53] From the stress-strain curves shown in Fig. 8, it is obvious that the toughness of MH-4scLAO/2CLOs is much higher than that of MH4scLAO.

Fig. 9 shows tensile strength, modulus and elongation at break in addition to tensile toughness which was calculated from the area of a stress-strain curve. Their values and standard deviations are summarizaed in Table S1. It was previously reported that a linear sc-PLA film with M_w from 1×10^5 to 1×10^6 surpassed the corresponding PLLA or PDLA films in tensile strength, Young's (tensile) modulus and elongation at break.[9,11] In this case, although tensile strength (34.7 MPa) and elongation at break (2.9 %) of MH4scLAO were comparable to those (28-40 MPa and 1.8-6.1%) of MH4LLAO and MH4DLAO, the former tensile modulus (1695 MPa) was lower than the latter ones (2355-2716 MPa). It is noteworthy that the tensile strength and modulus of MH4scLAO are comparable to those (45 MPa and 1820 MPa) of sc-PLA with M_w 1.3×10^6.[9] Although tensile strength and modulus of MH-4scLAO/2CLO decreased with increasing MH2CLO content, elongation at break and tensile toughness increased with MH2CLO content. Especially, tensile toughness (7.82 MJ m^{-3}) of MH-4scLAO/2CLO 50/50 was 11 times higher an average tensile toughness (0.71 MJ m^{-3}) of MH4LLAO and MH4DLAO. It is known that a linear sc-PLA with a M_w not higher than 5×10^4 has a high stereocomplexation ability, while is brittle, and that a linear sc-PLA with a M_w not lower than 1×10^5 displays a higher tensile strength and modulus than the corresponding hc-PLA does, while has a relatively lower stereocomplexation ability.[11] In a

similar manner, although H4scLAO with a molecular weight of ca. 4 500 had a high $\chi_{c,sc}$, it was a powder sample which hardly becomes a tough film. The macromolecular architecture for MH-4scLAO/2CLOs is effective to prepare tough films from a mixture of multifunctional star-shaped LLA and DLA oligomers which has a high stereocomplexation ability.

4. Conclusions

Stereoblock copolymer networks were prepared by reactions of H4LLAO, H4DLAO and H2CLO with MDI using a solution cast method. Thermal and mechanical properties of MH-4scLAO/2CLOs (100/0, 75/25, 50/50, 25/75 and 0/100) were compared with those of H4scLAO, MH4LLAO and MH4DLAO. Although H4scLAO was obtained as a powder sample, MH-4scLAO/2CLOs, MH4LLAO and MH4DLAO became relatively tough films. The formation of network structure by reactions of the hydroxy and isocyanate groups was confirmed by the FT-IR analysis and extraction experiment using chloroform. XRD analysis revealed that sc crystallites are preferentially formed for MH-4scLAO/2CLOs and H4scLAO, while hc crystallites are formed for H4LLAO and H4DLAO, and that MH4LLAO and MH4DLAO are amorphous. The melting temperatures of sc crystallites for MH-4scLAO/2CLOs were much higher than those of hc crystallites of H4LLAO and H4DLAO, while the values were slightly lower than that of H4scLAO. Although cold crystallization temperatures for MH-4scLAO/2CLOs were not observed during the first heating scan, but the temperatures were observed during the second heating scans after cooling at a rate of –100 °C min^{-1} from 230 (or 200) °C. No melting temperatures of hc crystallites were observed for MH-4scLAO/2CLOs in the first and second heating DSC curves. DMA analysis revealed that tan δ peak temperature of MH4scLAO is 78.2 °C, which is much higher than that (55.1 °C) for PLLA, and that the LAO and CLO segments are compatibilized for MH-4scLAO/2CLO 75/25. Elongations at break and tensile toughnesses of MH-4scLAO/2CLOs (75/25, 50/50 and 25/75) were much higher than those of MH4LLAO and MH4DLAO. The sc copolymer networks in this study are expected to be used as biodegradable and biocompatible materials requiring a higher toughness than that of PLA or sc-PLA.

Acknowledgements

We gratefully acknowledge financial support from the Chiba Institute of Technology. We thank Dr. Naozumi Teramoto and Dr. Toshiaki Shimasaki of our department for their helpful suggestions. We are also grateful to Mr. Ryusuke Osada of Material Analysis Center at the Chiba Institute of Technology for assisting in the XRD analysis reported here.

Notes and references

(1) X. Shi, Z. Chen and Y. Yang, *Eur. Polym. J.*, 2014, **50**, 243-248.

(2) L. Yu, K. Dean and L. Li, *Prog. Polym. Sci.*, 2006, **31**, 576-602.

(3) L. S. Nair and C. T. Laurencin, *Prog. Polym. Sci.*, 2007, **32**, 762-978.

(4) A. Bertin, *Macromol. Chem. Phys.*, 2012, **213**, 2329-2352.

(5) R. M. Rasal, A. V. Janorkar and D. E. Hirt, *Prog. Polym. Sci.*, 2010, **35**, 338-356.

(6) H. Liu and J. Zhang, *J. Polym. Sci. Part B: Polym. Phys.*, 2011, **49**, 1051-1083.

(7) X. F. Wei, R. Y. Bao, Z. Q. Cao, W. Yang, B. H. Xie and M. B.Yang, *Macromolecules*, 2014, **47**, 1439-1448.

(8) Y. Ikada, K. Jamshidi, H. Tsuji and S. H. Hyon, *Macromolecules*, 1987, **20**, 904-906.

(9) H. Tsuji, *Macromol. Biosci.*, 2005, **5**, 569-597.

(10) K. Fukushima and Y. Kimura, *Polym. Int.*, 2006, **55**, 626-642.

(11) H. Tsuji and Y. Ikada, *Polymer*, 1999, **40**, 6699-6708.

(12) N. Yui, P. J. Dijkstra and J. Feijen, *Macromol. Chem.*, 1990, **191**, 481-488.

(13) L. Li, Z. Zhong, W. H. Jeu, P. J. Dijkstra and J. Feijen, *Macromolecules*, 2004, **37**, 8641-8646.

(14) M. Hirata, K. Kobayashi and Y. Kimura, *J. Polym. Sci. Part A: Polym. Chem.*, 2010, **48**, 794-801.

(15) M. Hirata, K. Kobayashi and Y. Kimura, *Macromol. Chem. Phys.*, 2010, **211**, 1426-1432.

(16) N. Sugai, T. Yamamoto and Y. Tezuka, *ACS Macro Lett.*, 2012, **1**, 902-906.

(17) T. Isono, Y. Kondo, S. Ozawa, Y. Chen, R. Sakai, S. Sato, K. Tajima, T. Kakuchi and T. Satoh, *Macromolecule*, 2014, **47**, 7118-7128.

(18) T. Isono, Y. Kondo, I. Otsuka, Y. Nishiyama, R. Borsali, T. Kakuchi and T. Satoh, *Macromolecules*, 2013, **46**, 8509-8518.

(19) J. Shao, Z. Tang, J. Sun, G. Li and X. Chen, *J. Polym. Sci. Part B: Polym. Phys.*, 2014, **52**, 1560-1567.

(20) E. J. Shin, A. E. Jones and R. M. Waymouth, *Macromolecules*, 2012, **45**, 595-598.

(21) K. Fukushima, R. C. Pratt, F. Nederberg, J. P. K. Tan, Y. Y. Yang, R. M. Waymouth and J. L. Hedrick, *Biomacromolecules*, 2008, **9**, 3051-3058.

(22) T. Biela, A. Duda and S. Penczek, *Macromolecules*, 2006, **39,** 3710-3713.

(23) C. Hiemstra, Z. Zhong, L. Li, P. J. Dijkstra and J. Feijen, *Biomacromolecules*, 2006, **7**, 2790-2795.

(24) K. Nagahama, K. Fujiura, S. Enami, T. Ouchi and Y. Ohya, *J. Polym. Sci. Part A: Polym. Chem.*, 2008, **46**, 6317-6332.

(25) M. P. Shaver and D. J. A. Cameron, *Biomacromolecules,* 2010, **11**, 3673-3679.

(26) B. H. Tan, H. Hussain, T. T. Lin, Y. C. Chua, Y. W. Leong, W. W. Tjiu, P. K. Wong and C. B. He, *Langmuir*, 2011, **27**, 10538-10547.

(27) L. Calucci, C. Forte, S. J. Buwalda and P. J. Dijkstra, *Macromolecules*, 2011, **44**, 7288-7295.

(28) J. Shao, J. Sun, X. Bian, Y. Cui, G. Li and X. Chen, *J. Phys. Chem. B*, 2012, **116**, 9983-9991.

(29) S. J. Buwalda, L. Calucci, C. Forte, P. J. Dijkstra and J. Feijen, *Polymer*, 2007, **53**, 2809-2817.

(30) J. Shao, J. Sun, X. Bian, Y. Cui, Y. Zhou, G. Li and X. Chen, *Macromolecules*, 2013, **46**, 6963-6971.

(31) P. Purnama, Y. Jung and S. H. Kim, *Polym. Degrad. Stabl.*, 2013, **98**, 1097-1101.

(32) Y. Sakamoto and H. Tsuji, *Macromol. Chem.Phys.*, 2013, **214**, 776-786.

(33) H. Tsuji and M. Suzuki, *Macromol. Chem.Phys.*, 2014, **215**, 1879-1888.

(34) H. Tsuji and Y. Yamashita, *Polymer*, 2014, **55**, 6444-6450.

(35) D. J. A. Cameron and M. P. Shaver, *Chem. Soc. Rev.*, 2011, **40**, 1761-1776.

(36) H. Liu and J. Zhang, *J. Polym. Sci. Part B: Polym. Phys.*, 2011, **49**, 1051-1083.

(37) J. W. Park and S. S. Im, *J. Appl. Polym. Sci.*, 2002, **86**, 647-655.

(38) T. Yokohara and M. Yamaguchi, *Eur. Polym. J.*, 2008, **44**, 677-685.

(39) M. Shibata and Y. Inoue, *Polymer*, *2006*, **47**, 3557-3564.

(40) M. Shibata, N. Teramoto and Y. Inoue, *Polymer*, 2007, **48**, 2768-2777.

(41) R. Dell'Erba, G. Groeninckx, G. Maglio, M. Malinconico and A. Migliozzi, *Polymer*, 2001, **42**, 7831-7840.

(42) C. L. Simões, J C. Viana and A. M. Cunha, *J. Appl. Polym. Sci.*, 2009, **112**, 345-352.

(43) V. Vilay, M. Maratti, Z. Ahmad, K. Pasomsouk and M. Todo, *J. Appl. Polym. Sci.*, 2009, **114**, 1784-1792.

(44) R. Al-Itry, K. Lamnawar and A. Maazouz, *Polym. Degrad. Stabl.*, 2012, **97**, 1898-1914.

(45) M. H. Huang, S. Li and M.Vert, *Polymer*, 2004, **45**, 8675-8681.

(46) D. Cohn and H. Salomon, *Biomater.*, 2005, **26**, 2297-2305.

(47) Y. M. Kang, S. H. Lee, J. Y. Lee, J. S. Son, B. S. Kim, B. Lee, H. J. Chun, B. H. Min, J. H. Kim and M. S. Kim, *Biomater.*, 2010, **31**, 2453-2460.

(48) A. J. Nijenhuis, D. W. Grijpma and A. J. Pennings, *Polymer*, 1996, **37**, 2783-2791.

(49) H. M. Younes, E. Bravo-Grimaldo and B. G. Amsden, *Biomater.*, 2004, **25**, 5261-5269.

(50) R. S. Serra, J. L. Ivirico, J. M. M. Dueñas, A. A. Balado, J. L. G. Ribelels and M. S. Sánchez, *J. Polym. Sci. Part B: Polym. Phys.*, 2009, **47**, 183-193.

(51) Q. Liu, L. Jiang and L.Zhang, *Prog. Polym. Sci.*, 2012, **37**, 715-765.

(52) A. Shibita, H. Takase and M. Shibata, *Polymer*, 2014, **21**, 5407-5416.

(53) H. Takase, A. Shibita and M. Shibata, *J. Polym. Sci. Part B: Polym. Phys.*, 2014, **52**, 1420-1428.

(54) H. Bai, H. Liu, Bai, D.; Zhang, Q.; Wang, K.; Deng, H.; Chen, F.; Fu, Q. *Polym. Chem.* **2014**, *5*, 5985-5993.

(55) S. H. Kim, Y. K. Han, K. D. Ahn, Y. H. Kim and T. Chang, *Makromol. Chem.*, 1993, **194**, 3229-3236.

(56) S. H. Lee, S. H. Kim, Y. K. Han and Y. H. Kim, *J. Polym. Sci. Part A: Polym. Chem.*, 2001, **39**, 973-985.

(57) H. Korhonen, A. Helminen and J. V. Seppälä, *Polymer*, 2001, **42**, 7541-7549.

(58) E. S. Kim, B. C. Kim and S. H. Kim, *J. Polym. Sci. Part B: Polym. Phys.*, 2004, **42**, 939-946.

(59) H. Takase, K. Morita, A. Shibita and M.Shibata, *J. Polym. Res.*, 2014, **21**, 592(1-10).

(60) H. Tsuji, M. Nakano, M. Hashimoto, K. Takashima, S. Katsura and A. Mizuno, *Biomacromolecules*, 2006, **7**, 3316-3320.

(61) A. Petchsuk, S. Buchatip, W. Supmak, M. Opaprakasit and P. Opaprakasit, *eXPRESS Polym. Lett.*, 2014, **8**, 779-789.

(62) W. Hoogsteen, A. R. Postema, A. J. Pennings, G. T. Brinke and P. Zugenmaier, *Macromolecules*, 1990, **23**, 634-642.

(63) L. Cartier, T. Okihara and B. Lotz, *Macromolecules*, 1997, **30**, 6313-6322.

(64) T. M. Quynh, H. Mitomo, L. Zhao and M. Tamada, *J. Appl. Polym. Sci.*, 2008, **110**, 2358-2365.

(65) H. R. Pant, M. P. Neupane, B. Pant, G. Panthia, H. J. Oh, M. H. Lee and H. Y. Kim, *Colloids Surfaces B*, 2011, **88**.587-592.

(66) H. Tsuji and Y. Ikada, *J. Appl. Polym. Sci.*, 1996, **60**, 2367-2375.

(67) H. Tsuji and Y. Ikada, *J. Appl. Polym. Sci.*, 1998, **67**, 405-415.

Table 1 Data collected from the first heating DSC curves for all the samples.

Sample	$T_{g,LAO}$ (ºC)	$T_{m,CLO}$ (ºC)	$\Delta H_{m,CLO}$ (J g^{-1})	$T_{m,LAO}$ (ºC)	$\Delta H_{m,LAO}$ (J g^{-1})	$\chi_{c,LAO}$ (%)
H4LLAO	52.0	-	-	138.0	43.9	47.2
H4DLAO	59.8	-	-	138.7	37.0	39.8
MH4LLAO	77.9	-	-	-	0	0
MH4DLAO	73.8	-	-	-	0	0
H4scLAO	94.4	-	-	196.1	47.5	33.5
MH4scLAO	-	-	-	180.1	31.9	22.5
MH-4scLAO/2CLO 75/25	-	-	-	179.5	19.9	18.7
MH-4scLAO/2CLO 50/50	-	51.2	3.87	180.3	13.9	19.6
MH-4scLAO/2CLO 25/75	-	53.6	26.0	180.1	4.3	12.1
MH2CLO	(–29.3)[*1]	53.1	35.7	-	-	-

[*1] $T_{g,CLO}$

Table 2 Data collected from the second heating DSC curves of MH-4scLAO/2CLOs (100/0, 75/25, 50/50, 25/75 and 0/100).

Sample	$T_{g,CLO}$ (ºC)	$T_{m,CLO}$ (ºC)	$\Delta H_{m,CLO}$ (J g^{-1})	$T_{g,LAO}$ (ºC)	$T_{c,LAO}$ (ºC)	$\Delta H_{c,LAO}$ (J g^{-1})	$T_{m,LAO}$ (ºC)	$\Delta H_{m,LAO}$ (J g^{-1})	$\chi_{c,LAO}$ (%)
MH4scLAO	-	-	-	56.9	122.6	−19.2	167.4	10.1	7.1
MH-4scLAO/2CLO 75/25	-	-	-	51.0	90.2	−11.6	185.2	15.8	14.8
MH-4scLAO/2CLO 50/50	-	(45.2)	(5.4)	(-)[*1]	82.6	−3.5	187.1	13.0	18.3
MH-4scLAO/2CLO 25/75	−35.0	41.3	4.7	-	86.1	-	190.2	4.5	12.7
MH2CLO	−37.6	40.9	1.35	-	-		-	-	-
		52.0	0.41						

[*1] $T_{g,LAO}$ of MH-4scLAO/2CLO overlapped with $T_{m,CLO}$.

Figure and Scheme Captions

Scheme 1. Synthesis route of MH-4scLAO/2CLOs

Figure 1. FT-IR spectra of H4LLAO, MH-4scLAO/2CLOs (100/0, 75/25, 50/50, 25/75 and 0/100) and MDI.

Figure 2. XRD profiles of H4LLAO, H4DLAO, MH4LLAO and MH4DLAO.

Figure 3. XRD profiles of H4scLAO and MH-4scLAO/2CLOs (100/0, 75/25, 50/50, 25/75 and 0/100).

Figure 4. The first heating DSC curves of H4LLAO, MH4LLAO, H4scLAO and MH-4scLAO/2CLOs (100/0, 75/25, 50/50, 25/75 and 0/100).

Figure 5. The second heating DSC charts of MH-4scLAO/2CLOs (100/0, 75/25, 50/50, 25/75 and 0/100).

Figure 6. DMA curves of MH-4scLAO/2CLOs (100/0, 75/25, 50/50, 25/75 and 0/100).

Figure 7. TGA curves of H4LLAO, H4DLAO, MH4LLAO, MH4DLAO and MH-4scLAO/2CLOs (100/0, 75/25, 50/50, 25/75 and 0/100).

Figure 8. Stress-strain curves of MH-4scLAO/2CLOs (100/0, 75/25, 50/50, 25/75 and 0/100).

Figure 9. Tensile properties of MH4LLAO, MH4DLAO and MH-4scLAO/2CLOs (100/0, 75/25, 50/50, 25/75 and 0/100).

Electronic Supplementary Materials

Table S1 Tensile properties of MH4LLAO, MH4DLAO and MH-4scLAO/2CLOs (100/0, 75/25, 50/50, 25/75 and 0/100).

Fig. S1 400 MHz ^{1}H-NMR spectra of PER, DLA and H4DLAO in DMSO-d_6.

Fig. S2 400 MHz ^{1}H-NMR spectra of PERT, LLA, and H4LLAO in DMSO-d_6.

Fig. S3 FT-IR spectra of H4LLAO, H4DLAO, MH4LLAO, MH4DLAO and MDI.

Fig. S4 The first heating DSC curves of H4DLAO and MH4DLAO.

For Table of Contents

Stereocomplex formation in stereoblock copolymer networks composed of 4-armed star-shaped lactide oligomers and 2-armed ε-caprolactone oligomer

Mitsuhiro Shibata*, Masaya Katoh, Hayato Takase and Ayaka Shibita

Department of Life and Environmental Sciences, Faculty of Engineering,
Chiba Institute of Technology, 2-17-1, Tsudanuma, Narashino, Chiba 275-0016, Japan.
E-mail: mitsuhiro.shibata@p.chibakoudai.jp; Tel: +81 47 478 -423

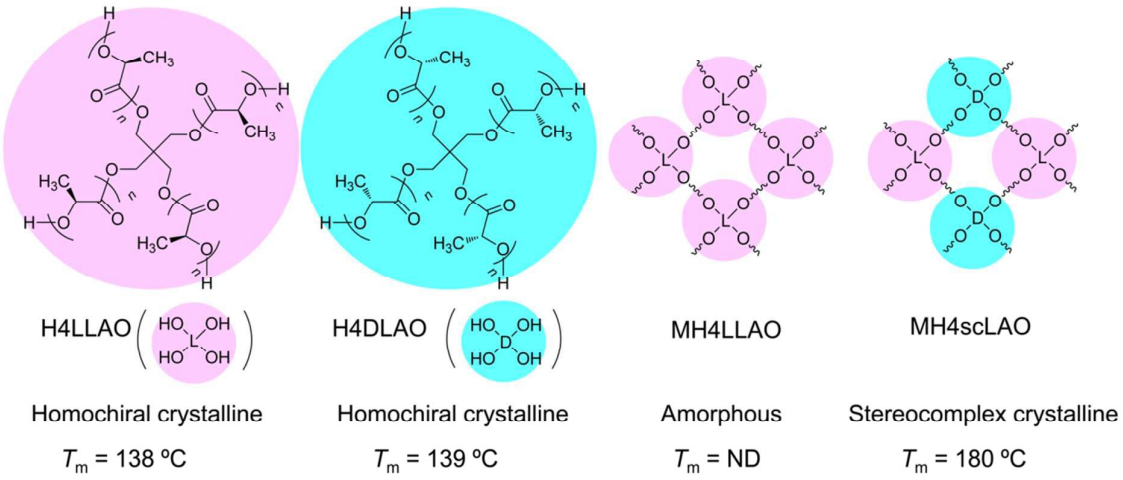

Stereoblock-copolymer network prepared from 4-armed star-shaped L-lactide and D-lactide oligomers formed stereocomplex crystallites, while the corresponding homochiral networks were amorphous. Incorporation of ε-caprolactone chain into the network improved the toughness.

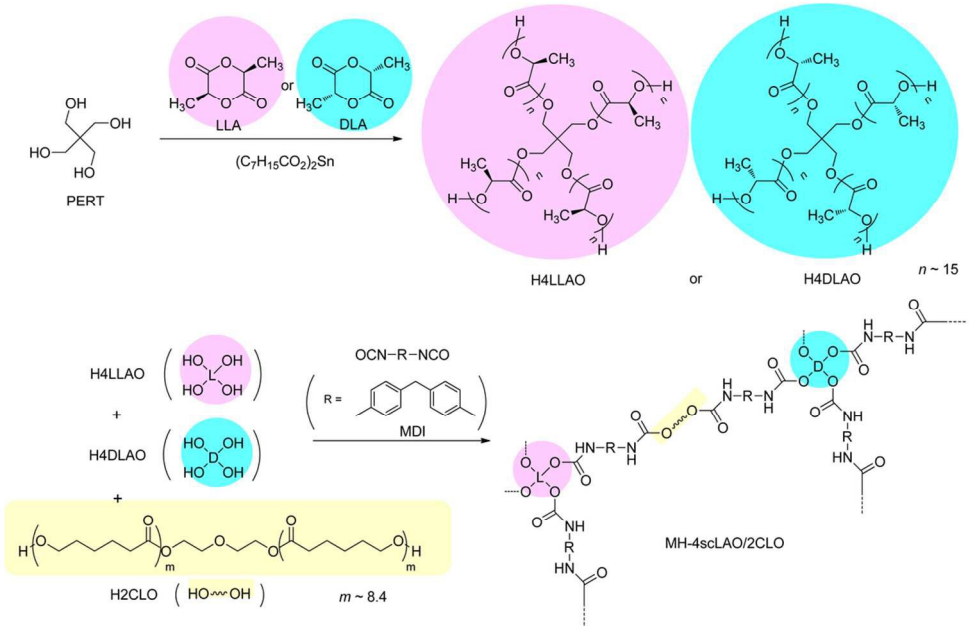

Scheme 1 Synthesis route of MH-4scLAO/2CLOs.
107x67mm (300 x 300 DPI)

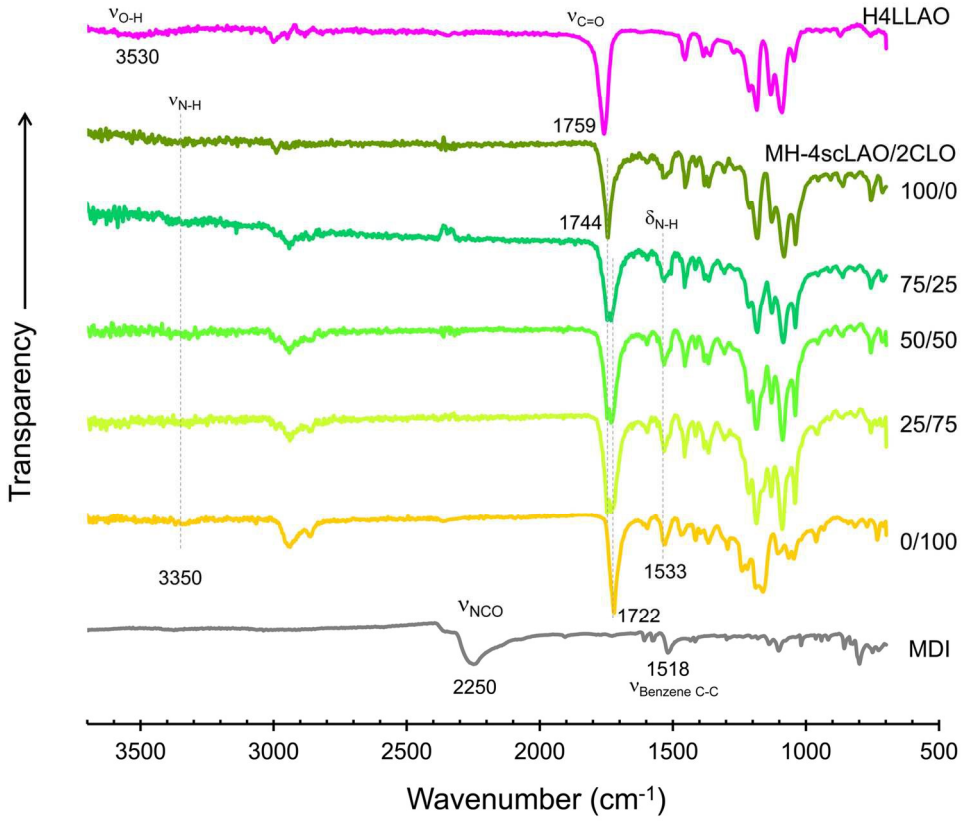

Fig. 1 FT-IR spectra of H4LLAO, MH-4scLAO/2CLOs (100/0, 75/25, 50/50, 25/75 and 0/100) and MDI.
141x117mm (300 x 300 DPI)

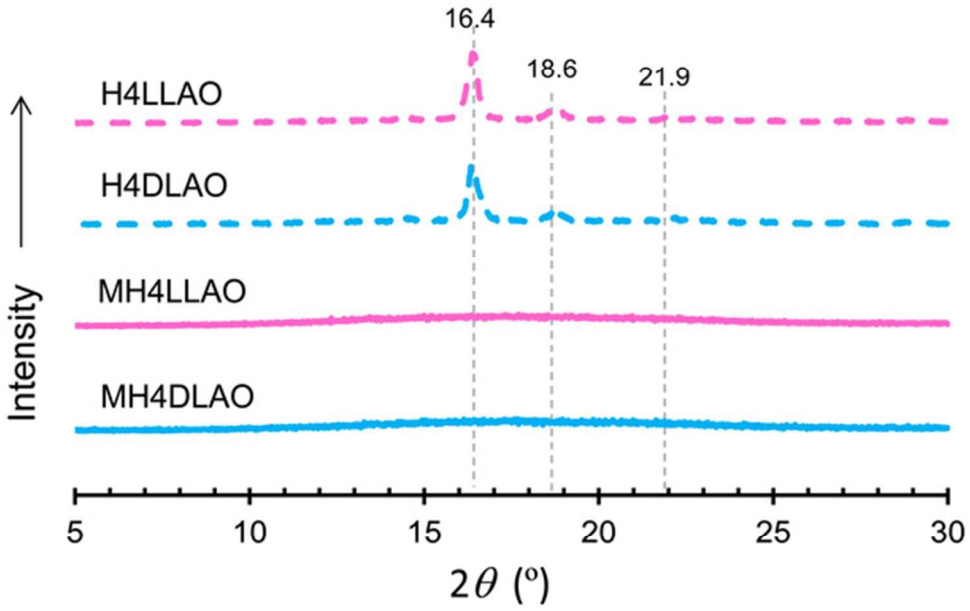

Fig.2 XRD profiles of H4LLAO, H4DLAO, MH4LLAO and MH4DLAO.
53x34mm (300 x 300 DPI)

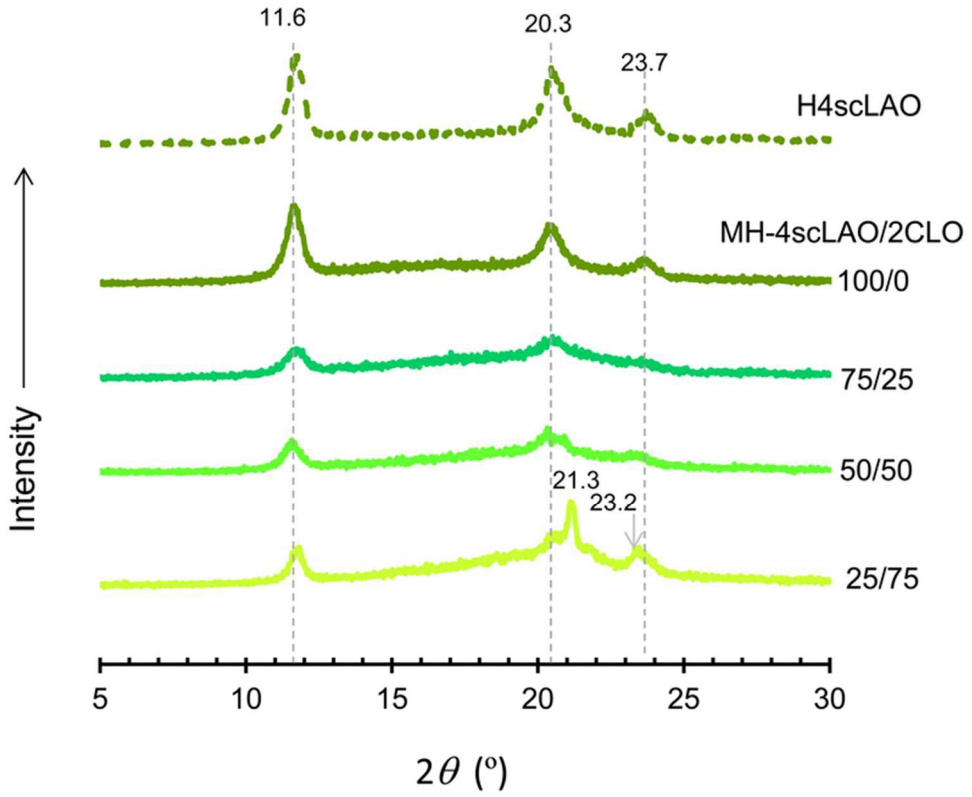

Fig.3 XRD profiles of H4scLAO and MH-4scLAO/2CLOs (100/0, 75/25, 50/50, 25/75 and 0/100).
69x59mm (300 x 300 DPI)

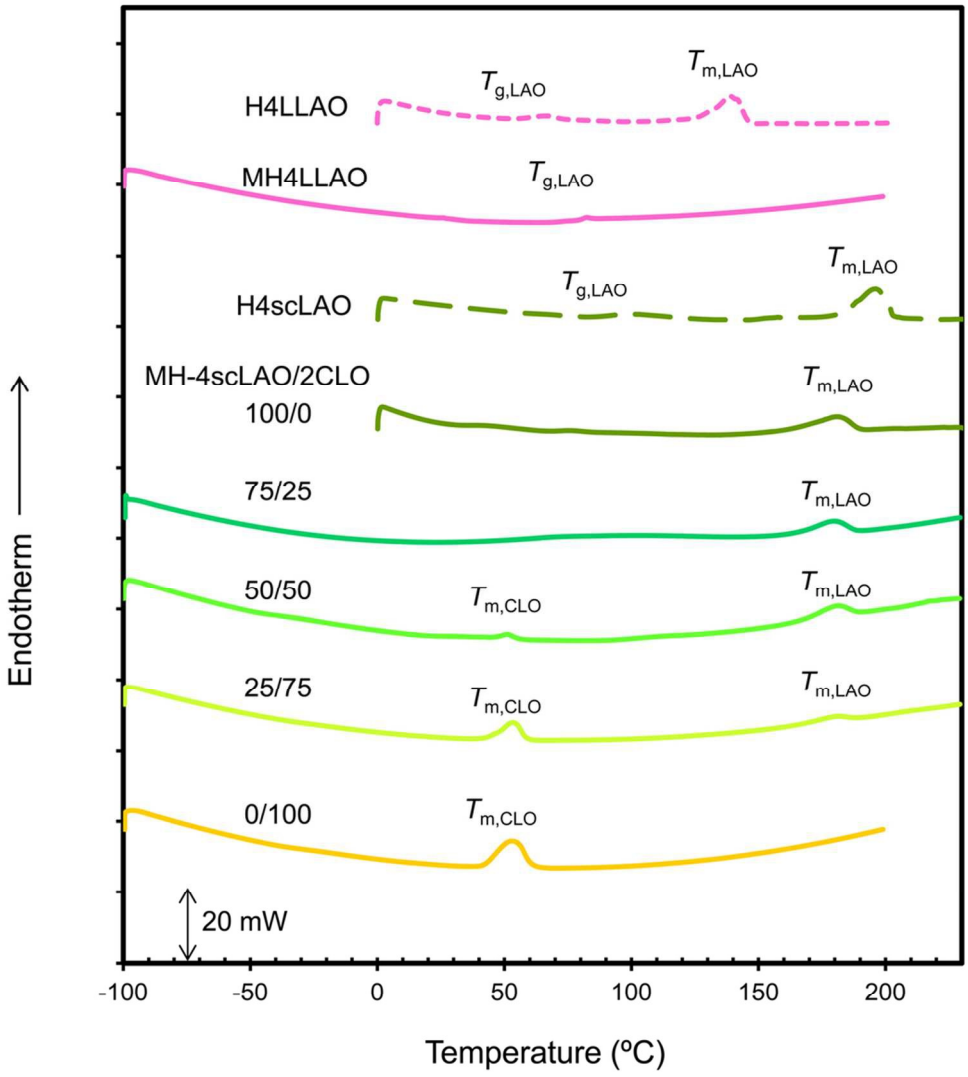

Fig.4 The first heating DSC curves of H4LLAO, MH4LLAO, H4scLAO and MH-4scLAO/2CLOs (100/0, 75/25, 50/50, 25/75 and 0/100).
91x101mm (300 x 300 DPI)

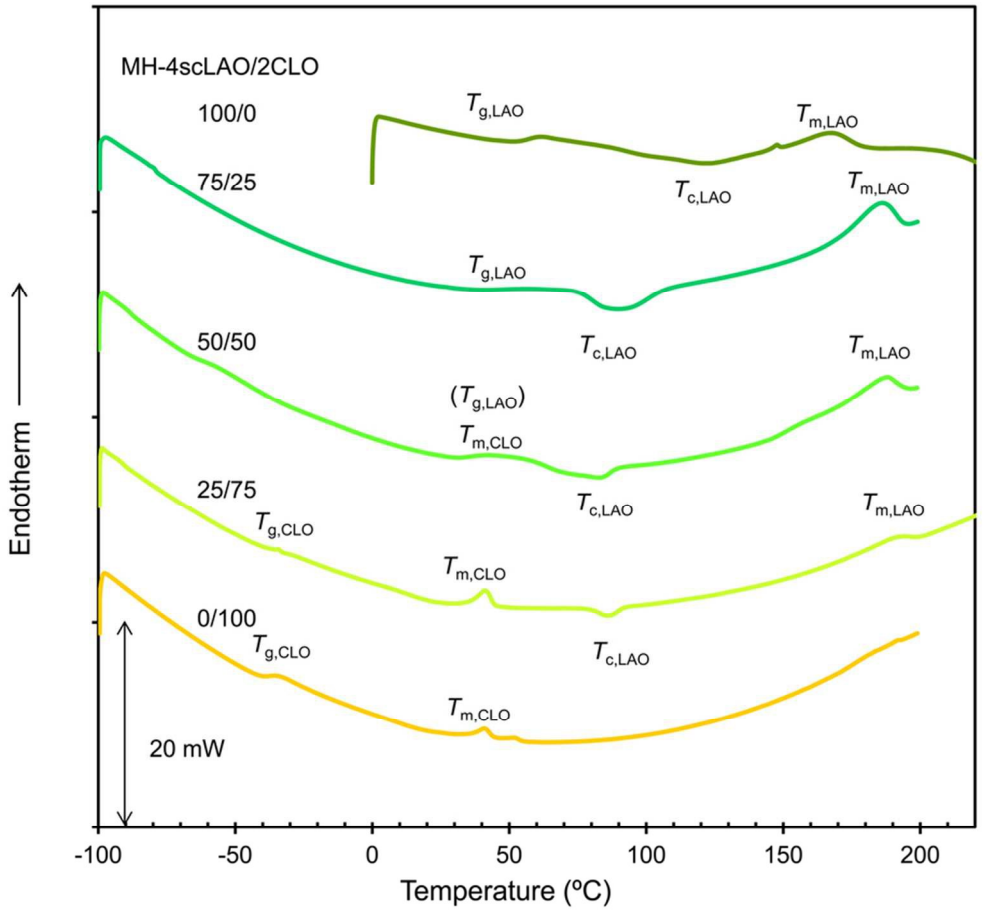

Fig.5 The second heating DSC charts of MH-4scLAO/2CLOs (100/0, 75/25, 50/50, 25/75 and 0/100).
78x75mm (300 x 300 DPI)

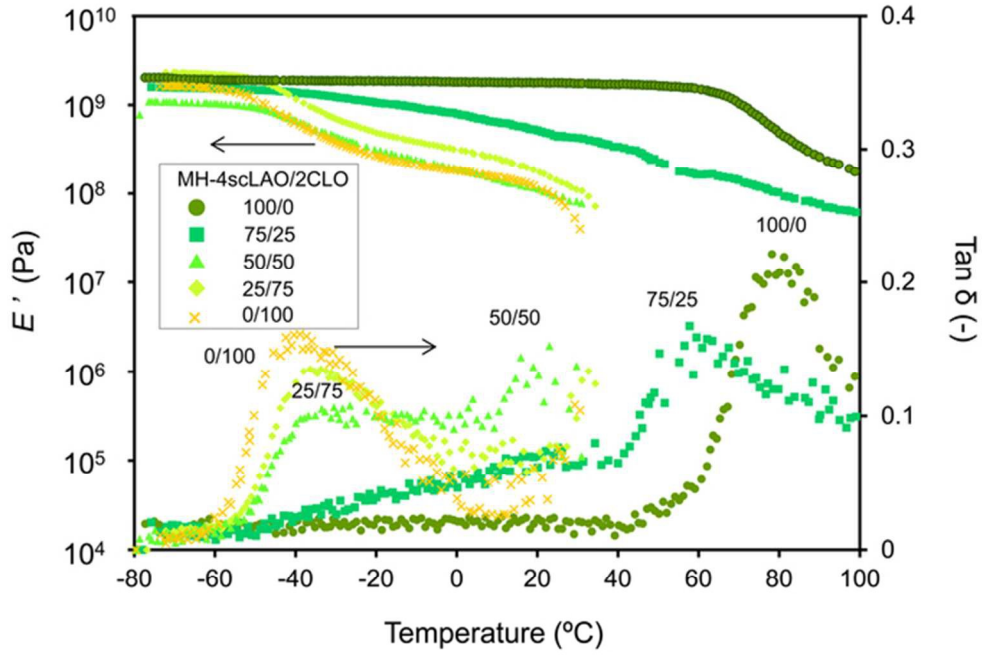

Fig.6 DMA curves of MH-4scLAO/2CLOs (100/0, 75/25, 50/50, 25/75 and 0/100).
58x42mm (300 x 300 DPI)

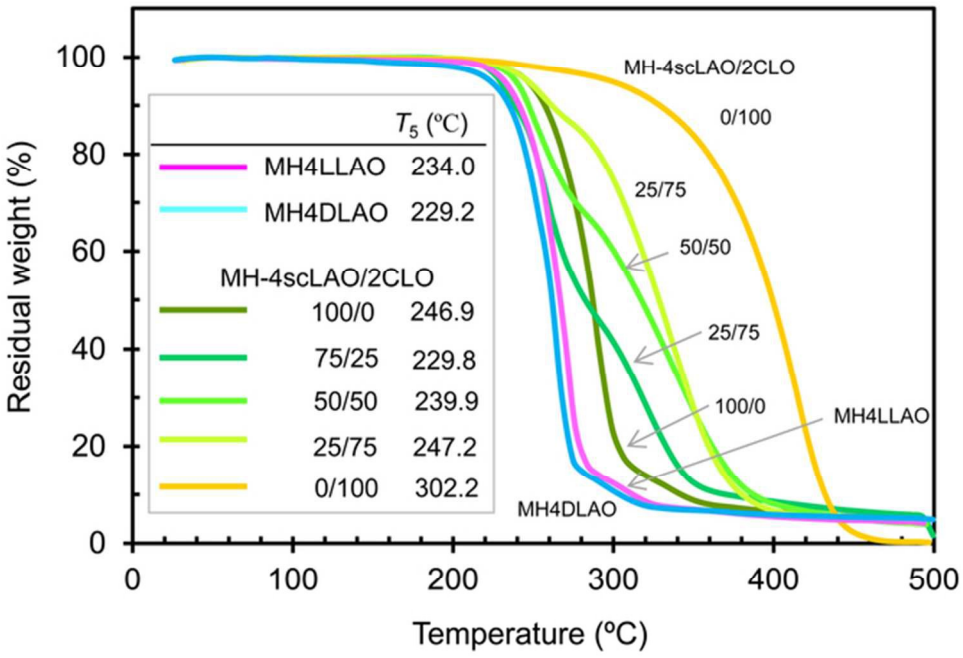

Fig.7 TGA curves of H4LLAO, H4DLAO, MH4LLAO, MH4DLAO and MH-4scLAO/2CLOs (100/0, 75/25, 50/50, 25/75 and 0/100).
58x41mm (300 x 300 DPI)

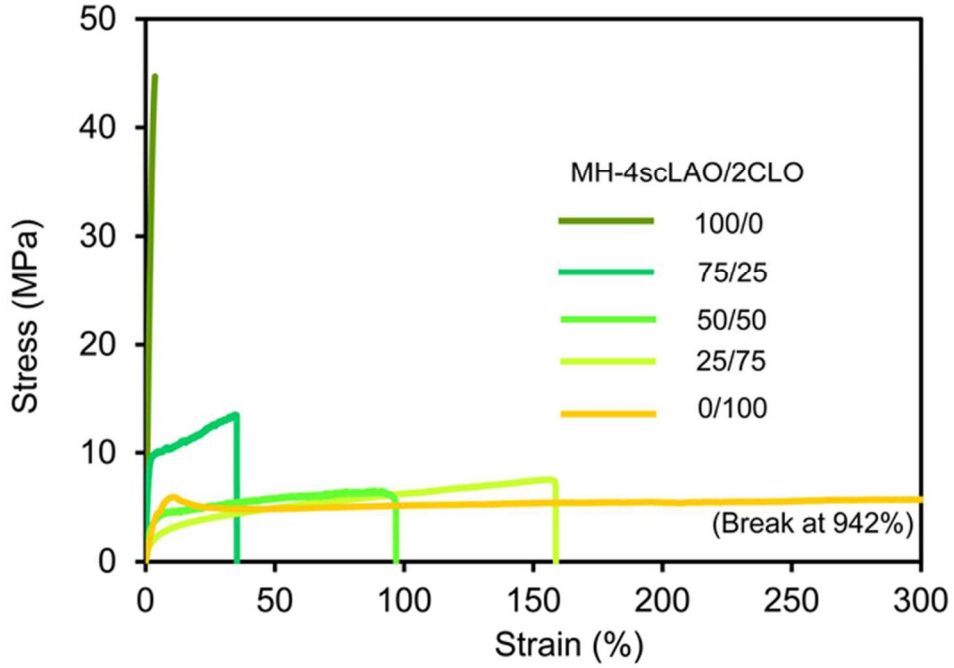

Fig.8 Stress-strain curves of MH-4scLAO/2CLOs (100/0, 75/25, 50/50, 25/75 and 0/100).
58x41mm (300 x 300 DPI)

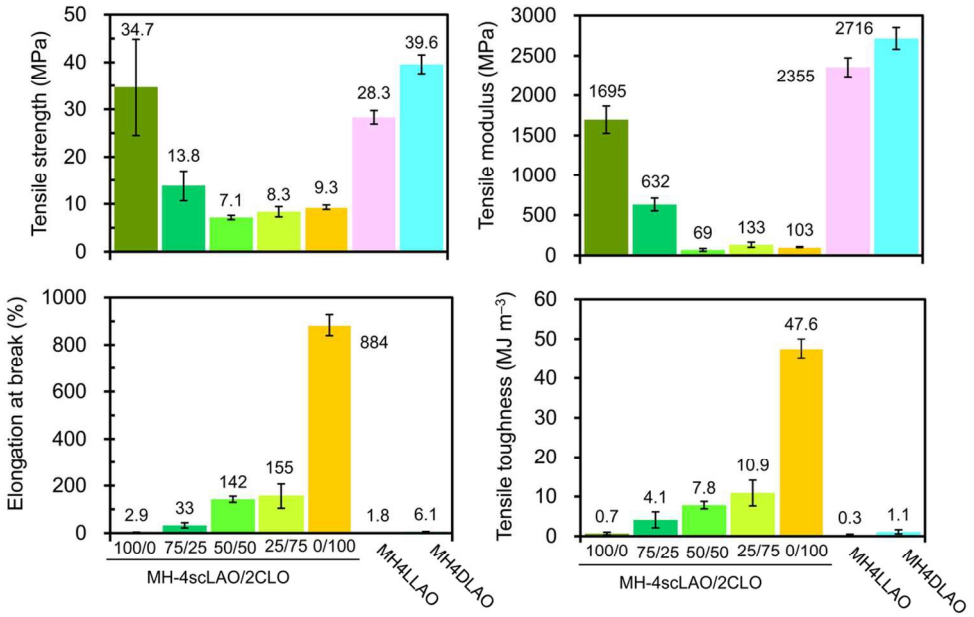

Fig.9 Tensile properties of MH4LLAO, MH4DLAO and MH-4scLAO/2CLOs (100/0, 75/25, 50/50, 25/75 and 0/100).
112x74mm (300 x 300 DPI)